AD-A208 032

(4)

AD

AD-E401 910

Contractor Report ARAED-CR-88015

COMBUSTION OF NITRAMINE AND NITRATE ESTER PROPELLANTS

Thieu H. Vu
Geo-Centers, Inc.
7 Wells Avenue
Newton Centre, MA 02159

Richard Field
Yvon Carignan
Project Engineers
ARDEC

DTIC
ELECTE
MAY 22 1989
E D
S

April 1989

U.S. ARMY ARMAMENT RESEARCH, DEVELOPMENT AND ENGINEERING CENTER

Armament Engineering Directorate

Picatinny Arsenal, New Jersey

US ARMY
ARMAMENT MUNITIONS
& CHEMICAL COMMAND
ARMAMENT RDE CENTER

89 5 22 061

REPORT DOCUMENTATION PAGE

1a. REPORT SECURITY CLASSIFICATION UNCLASSIFIED			1b. RESTRICTIVE MARKINGS		
2a. SECURITY CLASSIFICATION AUTHORITY			3. DISTRIBUTION/AVAILABILITY OF REPORT Approved for public release; distribution unlimited.		
2b. DECLASSIFICATION/DOWNGRADING SCHEDULE					
4. PERFORMING ORGANIZATION REPORT NUMBER GC-TR-88-1590			5. MONITORING ORGANIZATION REPORT NUMBER Contractor Report ARAED-CR-88015		
6a. NAME OF PERFORMING ORGANIZATION GEO-Centers, Inc.		6b. OFFICE SYMBOL	7a. NAME OF MONITORING ORGANIZATION ARDEC, AED		
6c. ADDRESS (CITY, STATE, AND ZIP CODE) 7 Wells Avenue Newton Centre, MA 02159			7b. ADDRESS (CITY, STATE, AND ZIP CODE) Energetics and Warheads Div (SMCAR-AEE) Picatinny Arsenal, NJ 07806-5000		
8a. NAME OF FUNDING/SPONSORING ORGANIZATION ARDEC, IMD STINFO Br		8b. OFFICE SYMBOL SMCAR-IMI-I	9. PROCUREMENT INSTRUMENT IDENTIFICATION NUMBER DAAA21-85-C-0139		
8c. ADDRESS (CITY, STATE, AND ZIP CODE) Picatinny Arsenal, NJ 07806-5000			10. SOURCE OF FUNDING NUMBERS		

			PROGRAM ELEMENT NO.	PROJECT NO.	TASK NO.	WORK UNIT ACCESSION NO.

11. TITLE (INCLUDE SECURITY CLASSIFICATION)

COMBUSTION OF NITRAMINE AND NITRATE ESTER PROPELLANTS

12. PERSONAL AUTHOR(S)

Thieu H. Vu, Geo-Centers, Inc., and Yvon Carignan and Richard Field, ARDEC Project Engineers

13a. TYPE OF REPORT Interim	13b. TIME COVERED FROM Jan 87 TO Mar 88	14. DATE OF REPORT (YEAR, MONTH, DAY) April 1989	15. PAGE COUNT 41

16. SUPPLEMENTARY NOTATION

17.	COSATI CODES		18. SUBJECT TERMS (CONTINUE ON REVERSE IF NECESSARY AND IDENTIFY BY BLOCK NUMBER)
FIELD	GROUP	SUB-GROUP	Nitramine Nitrate ester Double base propellant Burning rate
			Flame emissio Flame species Flame reactions Combustion

19. ABSTRACT (CONTINUE ON REVERSE IF NECESSARY AND IDENTIFY BY BLOCK NUMBER)

The burning rate of some nitramine and nitrate ester propellants has been measured as a function of the ambient gas composition and pressure. The presence of oxygen is most strongly felt at low pressures where further oxidation of the combustion gas enhances the burning rate by increasing heat release. However, at higher pressures, the burning rate is unaffected by oxygen. The overall flame chemistry has been found to follow 2nd- and 3rd-order rates for the nitrate ester and nitramine propellants, respectively. Emissions by carbon and CN from the combustions indicate that all these flames are fuel-rich with a predominantly RCN-type fuel. A number of flame reactions, with and without oxygen, have been considered to explain the spectra and the burning behavior of the propellants.

20. DISTRIBUTION/AVAILABILITY OF ABSTRACT ☐ UNCLASSIFIED/UNLIMITED ☒ SAME AS RPT. ☐ DTIC USERS		21. ABSTRACT SECURITY CLASSIFICATION UNCLASSIFIED	
22a. NAME OF RESPONSIBLE INDIVIDUAL I. HAZNEDARI		22b. TELEPHONE (INCLUDE AREA CODE) AV880-3316	22c. OFFICE SYMBOL SMCAR-IMI-I

DD FORM 1473, 84 MAR

TABLE OF CONTENTS

LIST OF FIGURES

LIST OF TABLES

INTRODUCTION

For several years, the application of optical methods to propellant combustion studies has been implemented at the U. S. Army ARDEC. Past work in this project has concentrated on the study of model flames and air-supported propellant combustion by coherent anti-Stokes Raman scattering (CARS) and high-speed photography (Refs. 1-10). These studies have demonstrated the capabilities to provide details of the flame temperature and products. The work reported here represents the next logical step in the project: an investigation of the behavior of propellants under more realistic conditions, particularly those simulating the ballistic pressures under which propellants are used.

A recent survey of the literature has been compiled on the study of solid propellant combustion (Ref. 11). In general, these studies can be divided into two groups. The first group emphasizes the physical and thermal aspects of the burning processes, but pays little attention to the chemical events attending those combustions. This is understandable since all the models of propellant combustion so far cannot handle all the detailed reactions in both the gas and condensed phases (Ref. 12). The second group includes those studies of the species distribution in the flame (Refs. 13, 14) and of the decomposition mechanism of the major propellant ingredients in their neat state (Ref. 15). These studies dwell more on the chemistry but make no connection to the bulk behavior of the propellant, such as the burning rate or flame spreading. The present work is an attempt to relate some of the phenomenology observed in the propellant combustion with the molecular events in the flame.

For that purpose, the work combines two simple techniques which can be applied simultaneously on each propellant burning. The first one is a convenient way to extract the burning rate and determine the flame zones: straightforward video recording of the combustion. The second technique is to identify the reactive flame species by their UV-visible emissions. This last method has often been done in the UV-IR region to trace the species profile in propellant flames, with the ultimate goal of explaining the temperature profile in terms of the molecular events, or vice versa (Refs. 13, 14, 16). Emission spectroscopy has also been used to compare the atomic and molecular constituents of the propellant flame with those of the burner flame, thus defining the propellant combustion in terms of the more tractable model flame (Ref. 17).

What is still lacking is a more comprehensive understanding of the relationship between the condensed phase burning rate and the chemistry in the gas phase. A propellant combustion consists of two stages:

-decomposition at the propellant surface, usually described by the pyrolysis of pure nitramine, nitrocellulose, or some simpler nitrate ester, and

-gas reactions, similar to those occurring in model flames.

1

Connecting the two stages is the heat generated by the flame chemistry which contributes to further surface decomposition. Thus, an understanding of the flame events is necessary to explain the processes at the burning surface. Moreover, the interaction of the burning surface and its flame with the reactive atmosphere is very rarely investigated. This is not surprising, considering the complexity dealt with even for propellants burned in inert atmospheres. Nevertheless, this participation of the ambient atmosphere cannot be ignored in real situations, such as in gun chambers. This report addresses the combustion of propellants under high pressures of both inert and reactive atmospheres. While a complete explanation and correlation of the bulk and microscopic behaviors is still a long-range goal and requires more work than what has been accomplished, a number of questions have been resolved and reported here. Other questions will inevitably be raised, which will help direct future work.

EXPERIMENTAL

Materials

All the propellants studied are representative nitramine and nitrate esters. The nitramine propellants are designated LOVA-1 and LOVA-2. The nitrate ester propellants consist of two types. The propellants based on nitrocellulose and metriol-trinitrate (NC/MTN) are designated NOSOL and Pb-NOSOL (lead catalyzed). The propellants based on nitrocellulose and nitroglycerine (NC/NG) are designated DB-1 and DB-2. Their sizes and compositions are listed in Table 1.

Experimental Setup

The system set up to perform simultaneous video recording and emission spectroscopy of propellant combustion is shown in Figure 1. The sample cell is a stainless steel optical bomb (Atlantic Research Corporation, Model 105) used in an earlier work (Ref. 9) and, depending on the thickness of the windows, can hold up to 340 atm (5000 psi). However, for the purpose of this work a rupture disk with a limit of 68 atm (1000 psi) is attached to the gas exhaust port of the cell to prevent an excessive pressure buildup. The removable bomb head serves a dual purpose: to suspend the sample holder at a pre-determined height in the bomb, and to conduct electrical leads to the nichrome ignition wire. A scale marker of known length is fixed to the sample holder to measure the distance travelled by the regressing surface of the propellant in each burning.

The gas flow in the cell is vertical upward to minimize the vacillation of the flame and to prevent coating of the cell windows by the flame products. The pressure in the bomb is maintained by adjusting the inlet and exhaust rates. A pressure transducer (Heise, Model 620) is attached to the gas line near the cell to monitor the pressure variation in the bomb for each burning. A Nicolet oscilloscope (Model 2090-III) stores the pressure-time records on disks.

A basic Panasonic system was used for video recording, consisting of a Model AG-1950 recorder player capable of still frame and slow-motion playback, a color monitor (Model MT-1340G) and a Digital 5000 camera with adaptable lenses. A few experiments had to incorporate a neutral density filter to prevent saturation on the camera by the intense flame. The spectroscopy setup was an optical multichannel analyzer (OMA) similar to one used previously (Ref. 10). The only difference here is in the OMA-III system (EG&G, Princeton Applied Research). With this system, monitoring the evolution of an emission band is made possible by storing successive detector scans into sequential memories. This operational mode allows fast scanning through

3

Table 1. Composition (weight %) and size of propellants

	LOVA-1[a]	LOVA-2[b]	NOSOL	Pb-NOSOL	DB-1	DE-2
NC	4[c]	4[c]	45.8[d]	47.5[e]	80.4[f]	80.4[f]
NG					18.3	18.3
MTN			41.0	39.4		
RDX	76	76				
TEGDN			10.1	10.0		
CAB	12	12				
Energetic plasticizer	2					
ATEC	7.6	5				
EC	0.4	1.0	1.1	1.0	1.3	1.3
Cryolite				1.0		
Lead Beta Resorcinate				1.0		
Potassium Sulfate			1.0			
Alcohol		0.04			3.65	3.04
Water		0.58			1.73	1.66
Acetone					3.01	2.63
Diameter (mm)	14	8.26	10.9	13.9	9.78	8.26

[a] Taken from Reference 1, [b] Nominal composition,
[c] 12.6% N, [d] 12.65% N, [e] 12.0% N, [f] 13.15% N

Abbreviations: NC = nitrocellulose, NG = nitroglycerin, MTN = metriol trinitrate,
TEGDN = triethylene glycol dinitrate, CAB = cellulose acetate butyrate,
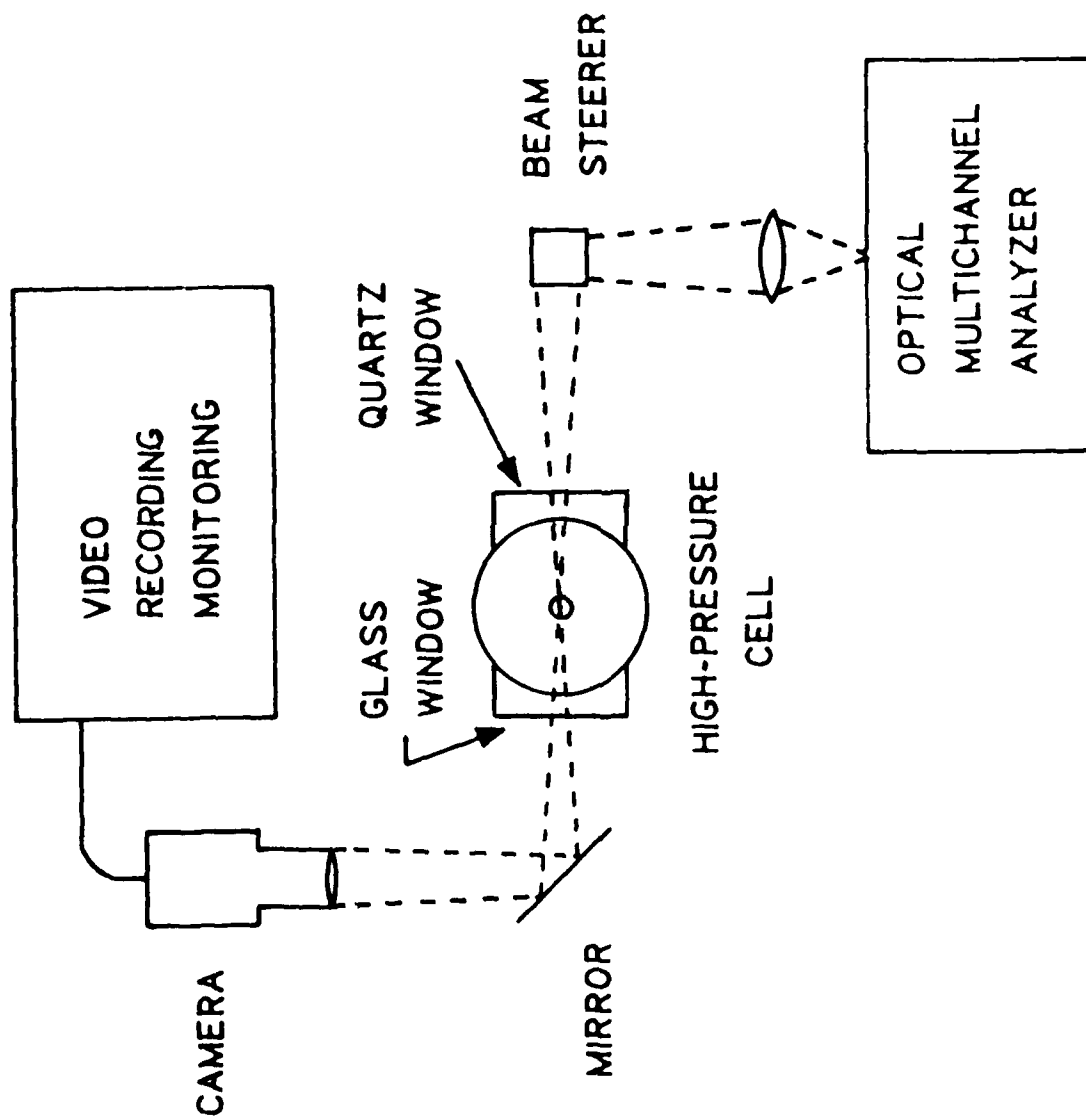ATEC = acetyl triethyl citrate, EC = ethyl centralite.

4

Figure 1. Experimental setup

the different combustion zones of a non-stationary flame during the regression of the burning surface. For this reason, an image rotator positioned between the cell window and the spectrograph serves to project a horizontal portion of the flame onto the detector slit.

PHENOMENOLOGICAL OBSERVATIONS

Flame Structure

Some general features expected of all propellant flames can be seen in Figures 2 and 3: end burning at a moderate pressure, the dark zone with a decreasing thickness as the pressure increases, and the luminous secondary flame. However, there are many features characteristic of each type of propellant and its burning conditions.

Nitramine Propellants

The secondary flame of both LOVA-1 and LOVA-2 propellants consists of two regions: adjacent to the dark zone is a bright white flame, probably with the hot flame products just formed; the second region is the equilibrium zone and has an orange color. An example of this is shown in Figure 2(a). Usually, as in Figure 2(b), parts of the luminous flame seem to hang on to the propellant. This is due to hot spots on the burning surface causing early reactions at or near the surface, which then emit luminous gas into the main secondary flame. When argon is used as the buffer gas, smoke can always be seen puffing out around the edge of the burning surface. At sufficiently low pressures when the pyrolysis mainly consists of decomposition and vaporization, long carbonaceous fibers start to form on the regressing surface of the propellant.

Figure 2(c) shows a LOVA-2 combustion in a Ar/O_2 buffer gas. In such an atmosphere, the LOVA combustion is always accompanied by flame spreading down the length of the propellant grain, thus clearly exposing the melt layer on the burning cone. The whole flame appears orange. Due to this spreading, the dark zone is not so clearly apparent, but can still be detected as a thin region surrounding the burning cone inside the flame. The smoke is not observable in these oxygen-supported combustions, especially as the O_2-content increases.

Nitrate Ester Propellants

NC/MTN Base. Both NOSOL and Pb-NOSOL propellants were studied in pure argon atmospheres only, between 7 and 20 atm (~ 100-300 psi). The combustion occurred in the end-burning fashion, without any flame spreading.

The NOSOL propellant shows a long bright white vertical flame with a violet tint, as can be seen in Figure 3(a). Spherical
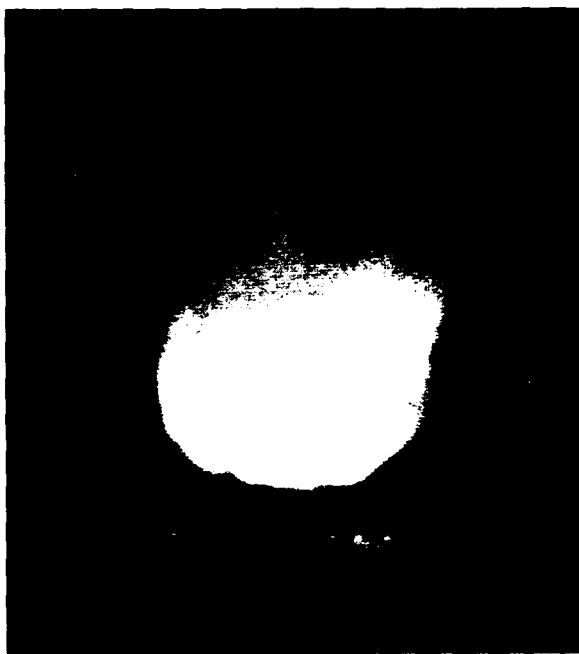
(a)
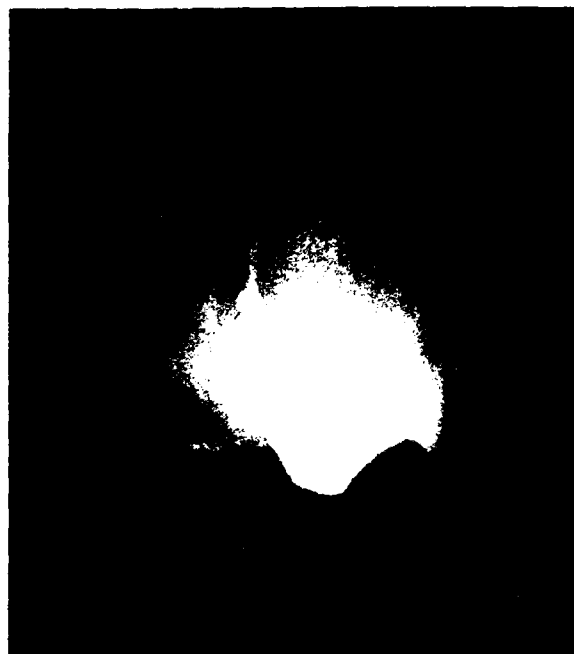
(b)

(c)

Figure 2. LOVA flame in Ar (a and b), and in Ar/O_2 (c)
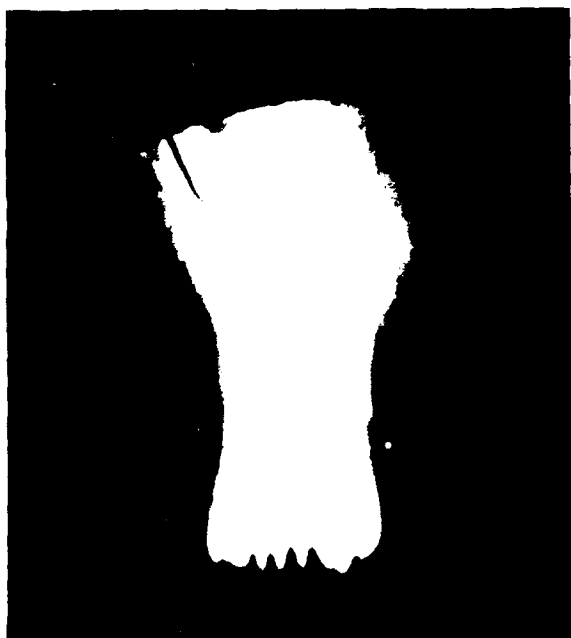
(a)
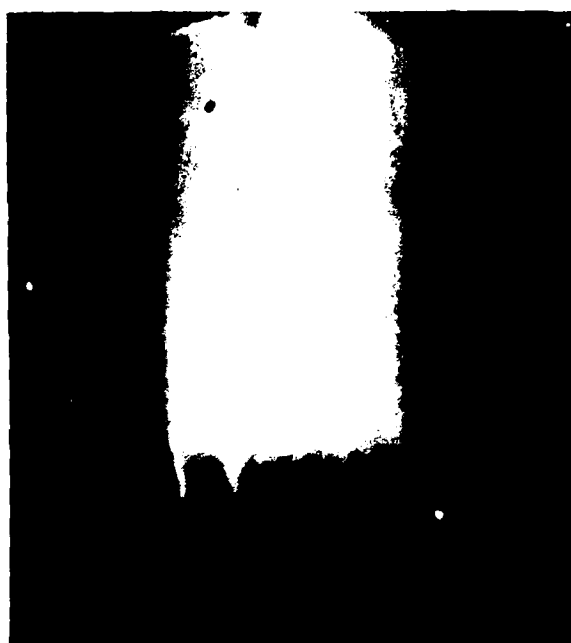
(b)

(c)

Figure 3. NOSOL (a), Pb-NOSOL (b) and DB-1 (c) flames in Ar

agglomerates were formed and got ejected from the burning surface. If they stayed on the surface, they became additional moving sources of luminous flame and sometimes even briefly carried parts of the flame when they ejected off the propellant. There is a dark zone in the NOSOL flame, although it is a little difficult to define because of the flame traces from the hot agglomerates.

Figure 3(b) shows the Pb-NOSOL propellant flame. There are some similarities and some contrasts between this flame and the NOSOL flame. The Pb-NOSOL flame has a more uniform orange-yellow color. At the low end of the pressure range, its combustion created large white solid clusters of various shapes, unlike those seen in the case of NOSOL. But as in the NOSOL combustion, some of these clusters can be seen as flame holders when they ejected or spilled off the propellant.

NC/NG Base. At low argon pressures both DB-1 and DB-2 propellants burn vertically downward, with glowing particles streaking upward from the horizontal burning surface. The flame always has a yellow-orange color, and is less stable than the NC/MTN flames. Increasing the pressure causes more flame spreading. This was observed in both Ar and Ar/O_2 gases, unlike the case of LOVA propellants where flame spreading occurs only in reactive atmospheres. The burning cone shows luminous spots on its surface; perhaps these were carbonaceous fibers or particles. Figure 3(c) shows an ill-defined dark zone, with its thickness increasing from the cone apex. Higher pressures cause such fast flame spreading that this dark zone can no longer be seen.

Burning Rate

The burning rates and the thickness of the dark zones were measured from the video recording of the burnings. Only slight pressure variations were observed during each experiment, the average value was taken as the constant pressure for each burning. Figure 4 shows a typical pressure-time history. The estimated variation is about 3-7% of the average pressure for the whole burning period (5-10 sec).

The log-log plots of burning rate, r, against pressure, P, were then fitted by linear regression-analysis to Vieille's equation,

$$r = a \cdot P^b \tag{1}$$

with r and P expressed in mm/sec and atm, respectively. In cases of flame spreading, the rate of flame spread, V was first measured and then converted to the burning rate by

$$r = V \cdot \sin\Theta \tag{2}$$
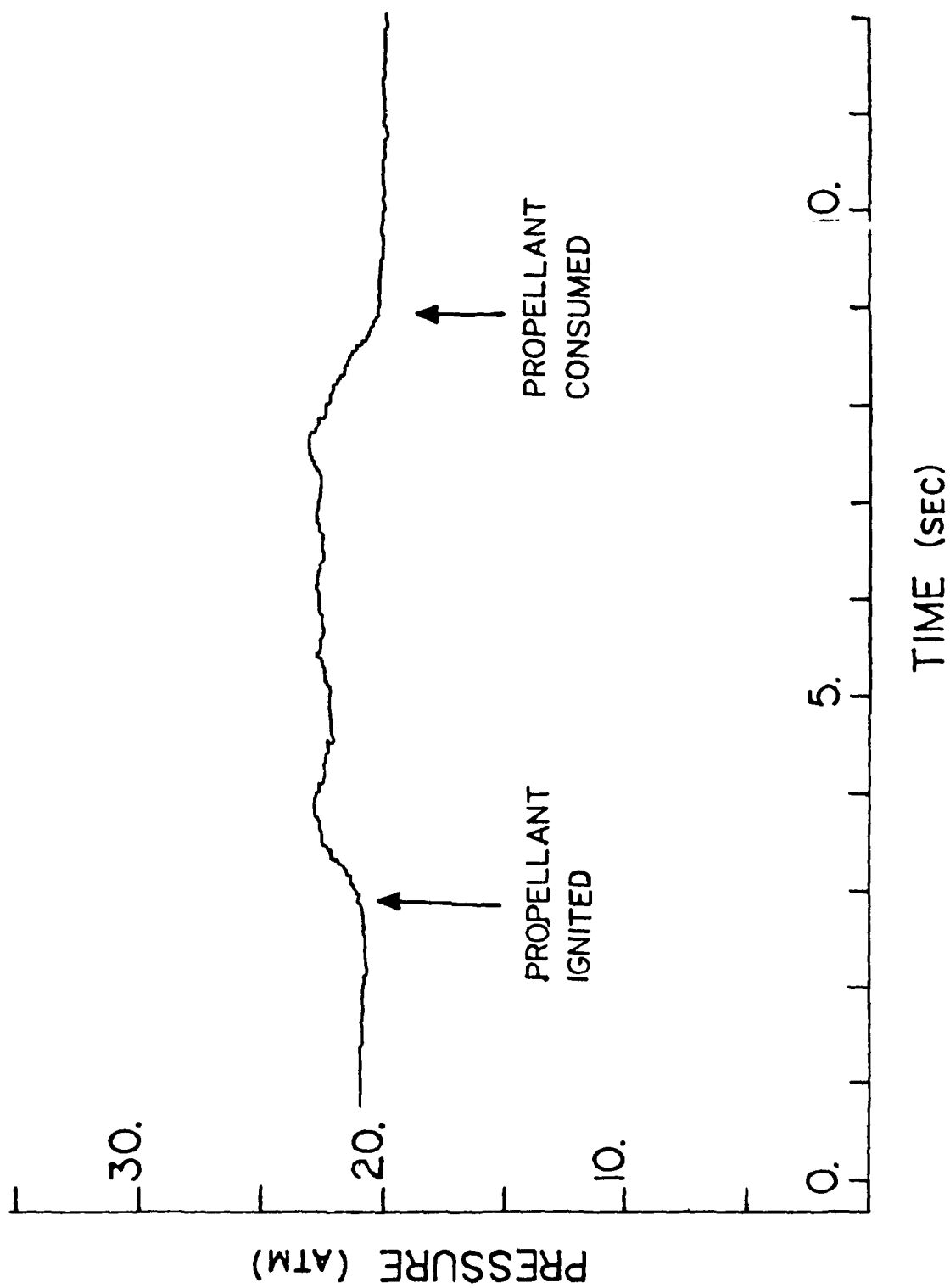
Figure 4. Chamber pressure during a propellant burning

11

with Θ = half-angle at the apex of the burning cone (Ref. 18). Figure 5 shows this relationship between the direction of flame spreading and the burning surface.
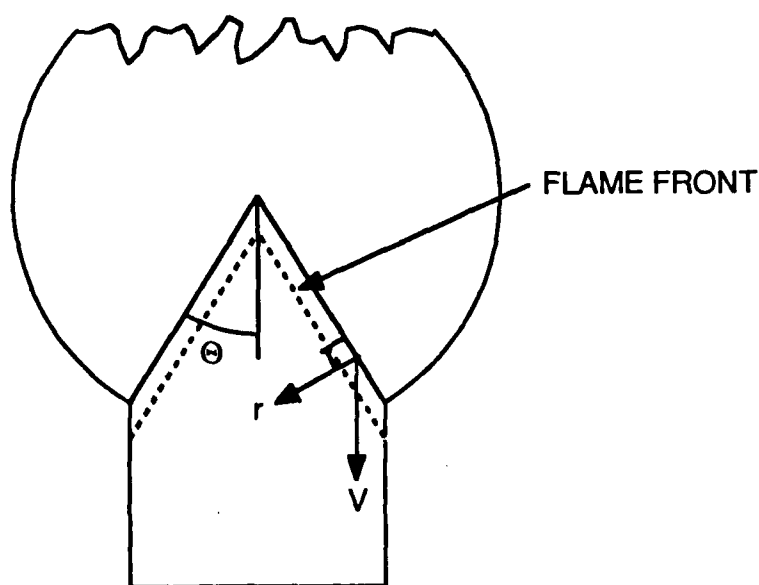
Figure 5. Directions of flame spreading and burning rate (adapted from Ref. 18)

Nitramine Propellants

Shown in Figure 6(a) is the burning rate of the LOVA-1 propellant in argon; it fits the rate law

$$r = 0.15 \cdot p^{0.70} \tag{3}$$

The LOVA-2 propellant burning in argon exhibits a more complicated behavior. As shown in Figure 7(a), its burning rate in argon rises sharply as the gas pressure increases from 6 atm (~90 psi) to 20 atm (~300 psi). Beyond that range, the burning rate levels off. Although this plot may be fitted to a single non-linear rate function, it will be more useful to consider two different pressure ranges and to apply Vieille's law to each:

$$r = 0.05 \cdot p^{1.18} \qquad \text{for} \quad 6 \text{ atm} < P < 20 \text{ atm} \tag{4a}$$
$$\text{and} \qquad r = 0.77 \cdot p^{0.25} \qquad \text{for} \quad 15 \text{ atm} < P < 50 \text{ atm} \tag{4b}$$

12
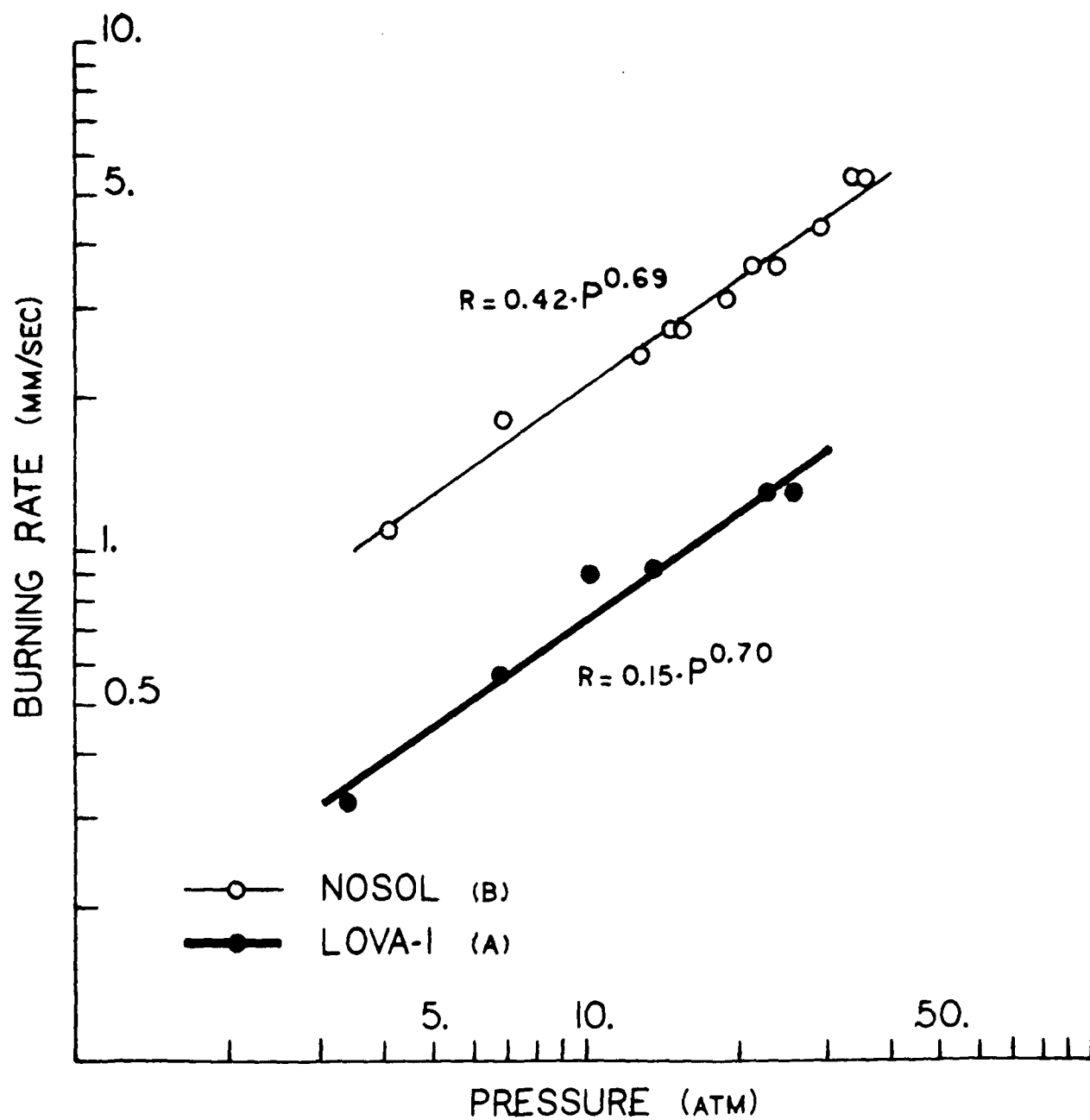
Figure 6. Burning rates of LOVA-1 and NOSOL propellants in Ar
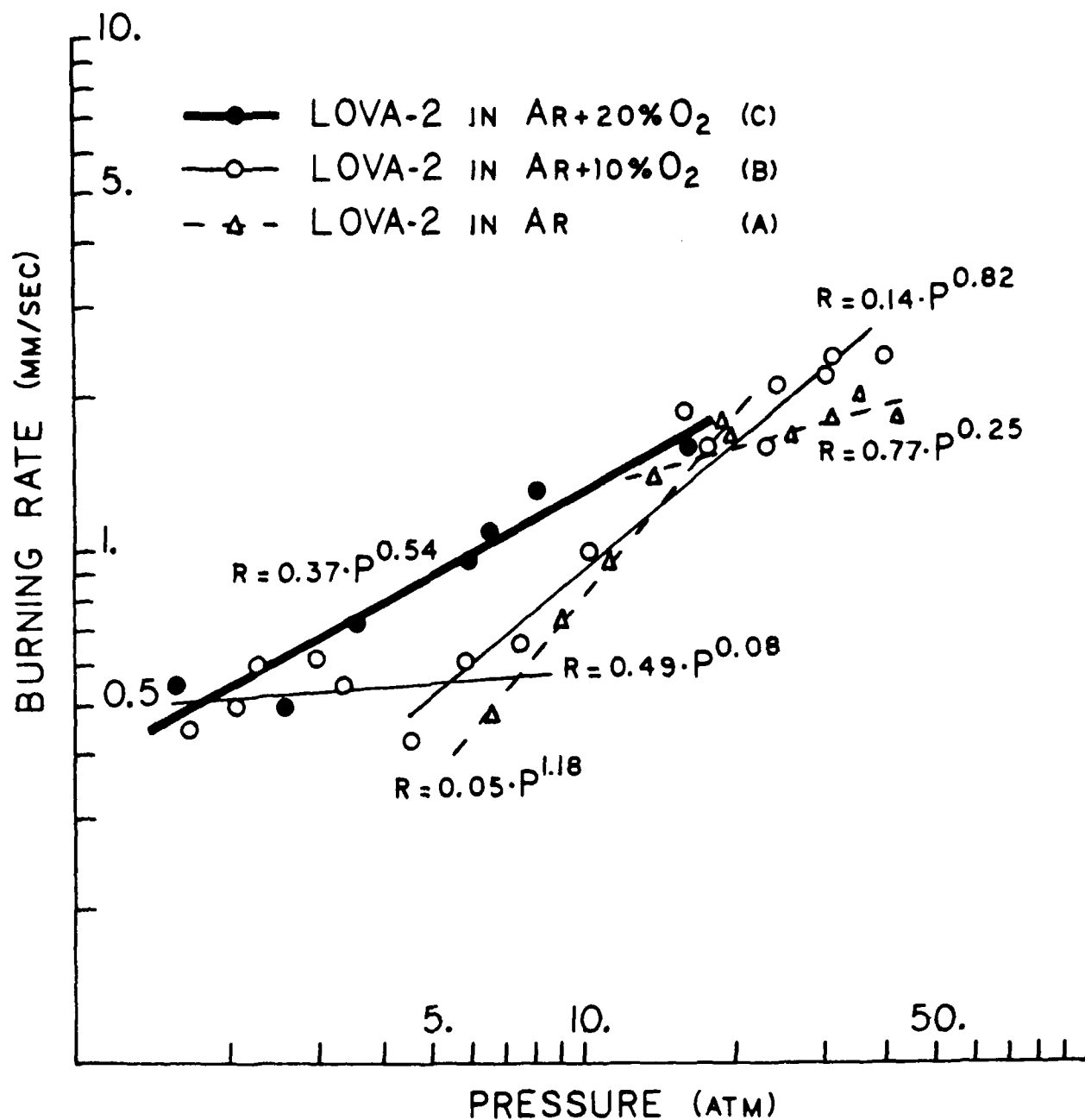
Figure 7: Burning rates of LOVA-2 propellant in Ar and in Ar/O_2 atmospheres

The presence of oxygen in the atmosphere significantly contributes to the burning rate, particularly at low pressures. For Ar + 10% O_2, the burning rate is non-zero but nearly constant at low pressures:

$$r = 0.49 \cdot P^{0.08} \qquad \text{for } 1 \text{ atm} < P < 6 \text{ atm} \qquad (5a)$$

However, as can be seen in Figure 7(b), at higher pressures the burning rate is almost the same as in pure argon, with the rate law

$$r = 0.14 \cdot P^{0.82} \qquad \text{for } 4 \text{ atm} < P < 50 \text{ atm} \qquad (5b)$$

Figure 7(c) shows the burning rate for LOVA-2 in Ar + 20% O_2. For the pressure range indicated in the figure, the rate law can be approximated by

$$r = 0.37 \cdot P^{0.70} \qquad (6)$$

The burning rate started out high near atmospheric conditions. But again, as the pressure becomes greater, it tends to get closer in value to the high pressure burning rate in argon.

Nitrate Ester Propellants

NC/MTN Base. All the double base propellants were found to react rapidly even in an inert surrounding. The Pb-NOSOL combustion was too fast to measure. Longer strands of this propellant would be needed to get any meaningful data. Thus, only the burning rate of the unleaded NOSOL propellant in argon was determined in this work:

$$r = 0.42 \cdot P^{0.60} \qquad (7)$$

Figure 6(b) simply illustrates the fact that the nitrate ester propellant consistently reacts faster than the nitramine propellant.

NC/NG Base. The burning rate of the DB-1 propellant was found to be

$$r = 0.33 \cdot P^{0.81} \qquad \text{in Ar} \qquad (8)$$
$$r = 0.34 \cdot P^{0.81} \qquad \text{in Ar + 5\% } O_2 \qquad (9)$$
$$r = 0.78 \cdot P^{0.60} \qquad \text{in Ar + 10\% } O_2 \qquad (10)$$

Apparently, the oxygen-content in the Ar + 5% O_2 mixture was not strong enough to affect the burning rate, although it did sustain the combustion at low pressures where the inert gas failed. Figure 8(d) and Equation 10 show the influence of O_2 more clearly, i.e. only at low pressures. At higher pressures the burning rates in reactive atmospheres
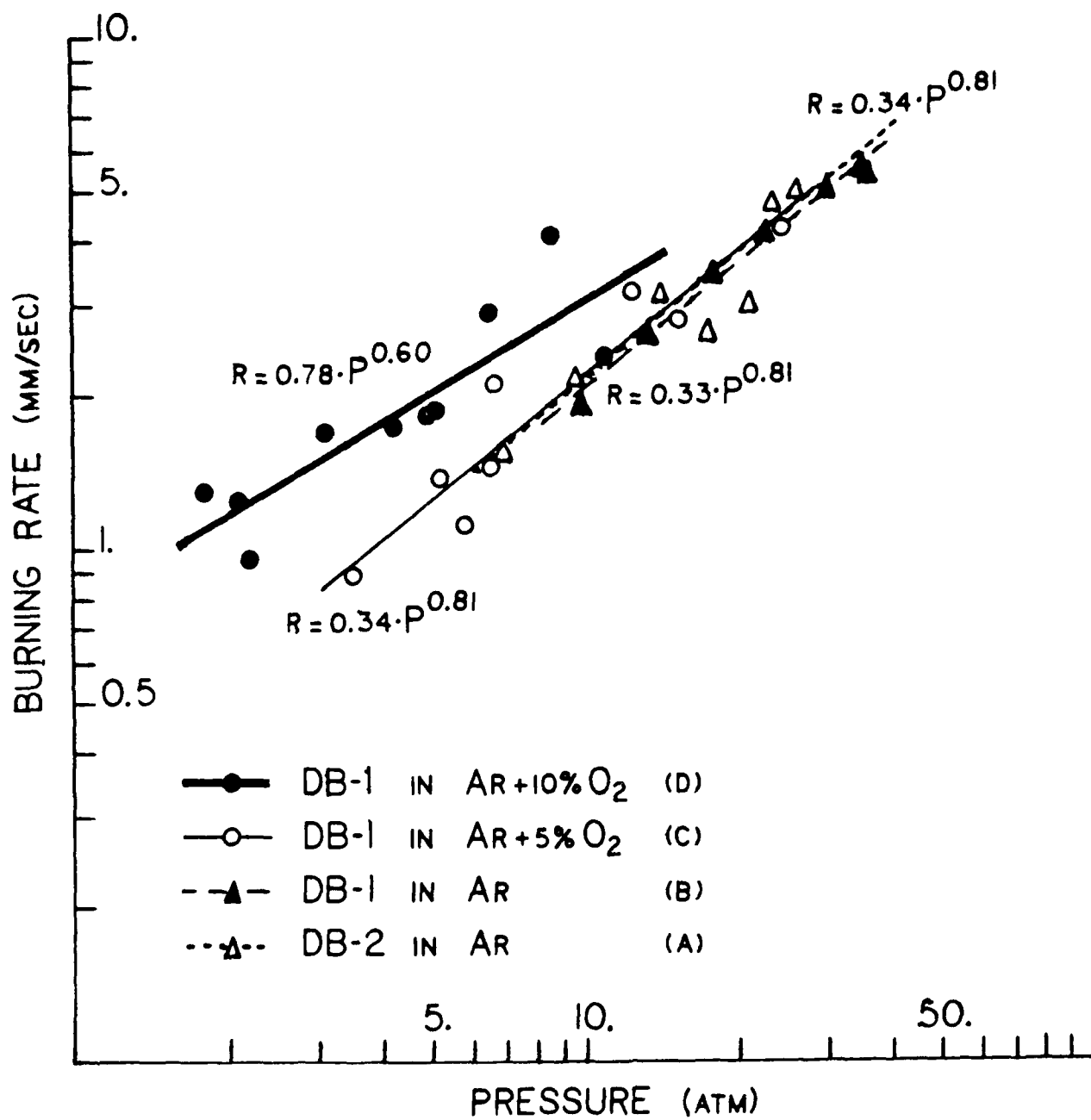
Figure 8. Burning rates of DB propellants in Ar and in Ar/O_2

and in inert gas approach each other and oxygen loses its rate-enhancing effect.

An examination of Figure 7(b) gives some insight into the burning behavior of the propellants at low Ar/O_2 pressures. Below 6 atm the burning rate is essentially independent of pressure, as also indicated by the near-zero exponent in Equation 5a. Apparently, the decomposition rate at the burning surface is unaffected by the thermal feedback from reactive collisions in the gas phase. It is interesting to note that, when enough O_2 is present in the atmosphere, all the pressure exponents in Vieille's law are smaller than in the cases where only an inert atmosphere is used. This is true until the high pressure region is reached, where the burning rates in Ar/O_2 mixtures and in pure argon are closer in their values.

Effect of Propellant Dimensions

To determine the effect of strand size of the propellant on its burning rate, the DB-2 propellant was tried in pure argon, giving the rate-law

$$r = 0.34 \cdot P^{0.81} \tag{11}$$

Within each other's experimental uncertainties, Equations 11 and 8 are exactly the same. It is clear that for the DB-1 and DB-2 propellants, the dimension of the strand does not affect the burning rate.

Order of the Overall Flame Reaction

Based on a model in which the dark zone serves as an induction volume where the gaseous species mix and react to give the final products in the secondary flame, N. Kubota and coworkers (Ref. 13) have proved that the order of the total reaction in the gas phase can be summarized by

$$n = b - d \tag{12}$$

where b is defined in Equation 1; and d is the exponent in the relation between the thickness of the dark zone, H_{dz}, and the pressure:

$$H_{dz} = c \cdot P^d \tag{13}$$

with c being a constant characteristic of the propellant and burning conditions. As mentioned earlier, the dark zone can be defined in these

17

experiments only when the end-burning mode allows an unambiguous visual measurement. This precludes the cases of flame spreading, such as often seen with the NC/NG propellants studied in this work. The values of H_{dz} for the LOVA and the unleaded NOSOL propellants have been determined and least-square fitted to the following equations:

$$H_{dz} = 731 \cdot P^{-2.36} \text{ for LOVA-1} \tag{14}$$
$$H_{dz} = 1026 \cdot P^{-1.93} \text{ for LOVA-2} \tag{15}$$
$$H_{dz} = 152 \cdot P^{-1.46} \text{ for NOSOL} \tag{16}$$

These fittings are shown in Figure 9. The orders of the overall flame reactions can now be obtained by applying the numerical values to b and d in Equation 12. A caution must be taken here concerning the b-value used for LOVA-2. It must be evaluated in the same pressure region as the corresponding d-value, i.e. Equation 4a. The results are listed here:

Table 2. Order of the overall flame reaction in argon

Propellant	b	d	n
LOVA-1	0.70	-2.36	~3
LOVA-2	1.18	-1.93	~3
NOSOL	0.69	-1.46	~2

In general, the chemistry in a propellant flame can be represented by

$$n_f \cdot \text{Fuel} + n_o \cdot \text{Oxidizer} \rightarrow \text{Final Products}$$
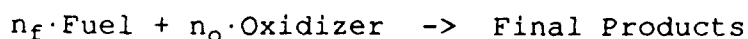
with n_f ant n_o being the stoichiometric coefficients. The fuel in the NOSOL flame should be an aldehyde, and the oxidizer NO_2 (Refs. 16, 20). The final products include H_2O, CO_2 and N_2, among others. Still to be determined are the stoichiometric coefficients. All the NOSOL and DB propellants, with nitrocellulose as their main ingredient, are expected to have the same n_f and the same n_o.

The chemistry in the LOVA flame is more involved, being a third order reaction. Moreover, much debate is still going on concerning the immediate products of nitramine decomposition (Refs. 15, 20). Basically, the uncertainty is on the evidence of the first bond breaking step of nitramines. Thus, the flame fuel can be either a RCHO or a RCN molecule, or both. The same can be said about NO_2 and N_2O in the oxidizer role.

Figure 9. Thickness of the dark zones as a function of pressure

19

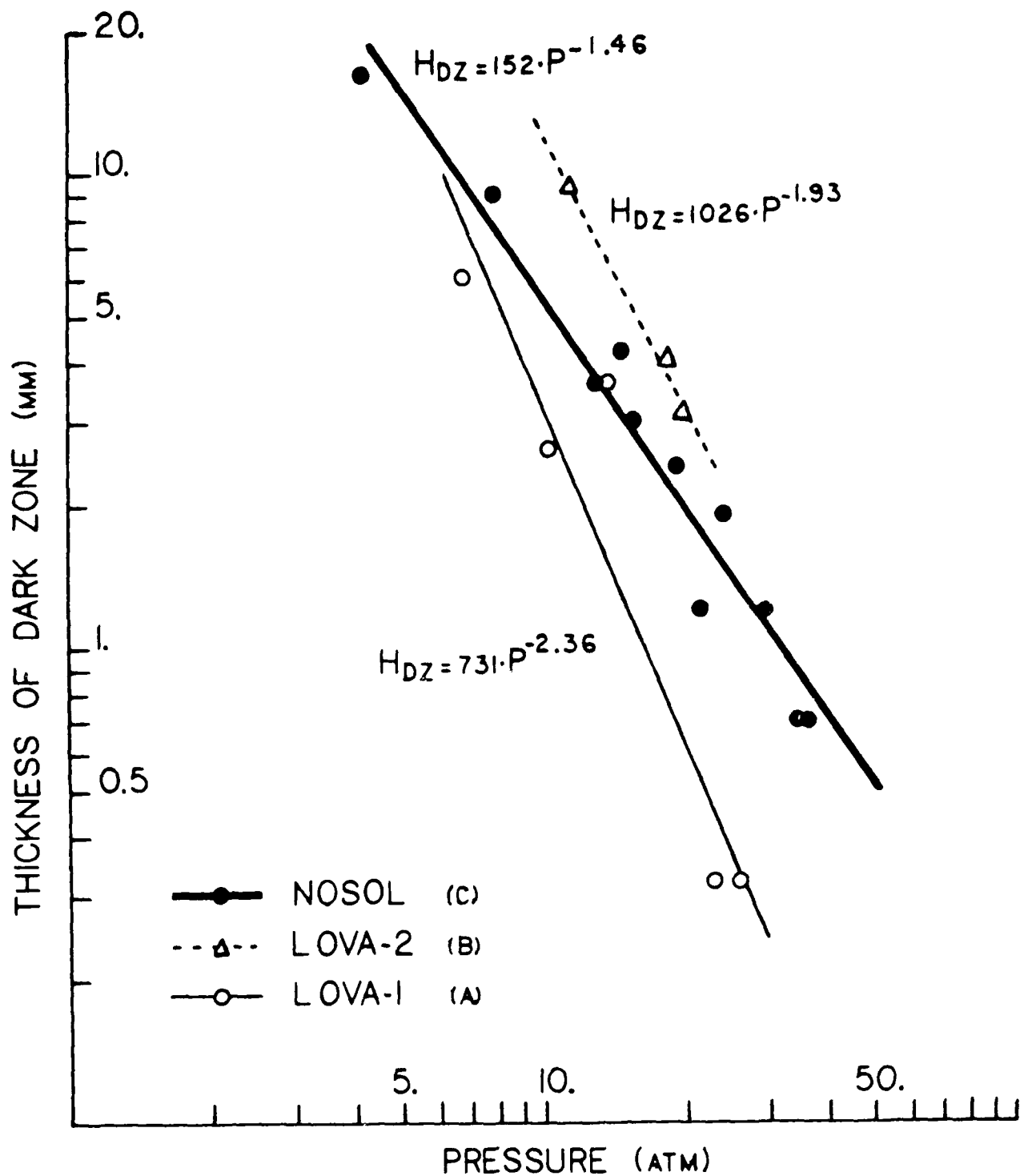A good knowledge of the gaseous participants is needed if an accurate overall reaction in the propellant flames is ever to be obtained. The next chapter on emission spectroscopy will discuss this aspect.

EMISSION SPECTROSCOPY OF PROPELLANT FLAMES

Propellant Flame Species

Most of the spectroscopy was done in an inert atmosphere to determine the species coming exclusively from the propellant components. However, a good number of spectra were also taken from the burnings in air or in an O_2-seeded atmosphere in order to evaluate the role of oxygen in the combustion chemistry. When the burning was done in the combustion chamber, the pressure was kept constant in the 14-20 atm (~200-300 psi) range. In spite of a strong background continuum in many spectra, signals from the common species expected of these flames can be easily recognized. Figures 10 and 11 are examples of the spectral quality obtained. Because of the high pressure in the optical bomb, the bands show collision-broadening.

All the propellants studied here produced C_2, CN, CO and NH in argon as well as in air. CO exhibited three main bands in argon. Detected early in the burnings were the emissions at 4661 and 5198 Å. The 3305 Å emission, of the Third Positive CO-bands, appeared strongly in the last half of the burning, apparently in the secondary flame. These Third Positive bands were unmistakably recognized by their violet-degraded structure. No CH-emission was found, except for a faint signal in one case of the air-supported LOVA-2 combustion. Also missing in all the combustions in argon were the emissions by OH. Table 3 summarizes the main results.

Other species may have occurred also but their signals were neither strong nor consistent enough to definitely prove their existence. Among these species are NO and N_2. A search was carried out for NO in the DB-1 and LOVA-2 flames, with negative results. Although a signal was recorded at 4284 Å in the DB-1 flame, it was too weak to be conclusive; it would be due to the NO γ-band. An emission at 4722 Å was detected from the Pb-NOSOL and LOVA-1 flames in argon. This could be due to $N_2(C^3\Pi_u)$. However, as indicated in Table 3, no emission was found at at that same wavelength in the case of the LOVA-2 and DB-1 flames in argon. A thermodynamic calculation of the propellant combustions studied here indicated that N_2 is a very insignificant product. Thus, the presence of N_2 as a propellant flame product, be it excited or equilibrated, still needs to be investigated further.

A number of emission bands suggested the ions CH^+ (4777 and 4797 Å) and CO^+ (4711 Å). Again the emission signals here are weak and broad. Moreover, the strong background continuum hampers any conclusive identifications. The ionization of flame species is usually highly endothermic, and it is doubtful that the propellant flames were hot enough to provide the energy necessary to strip the neutral species of

21
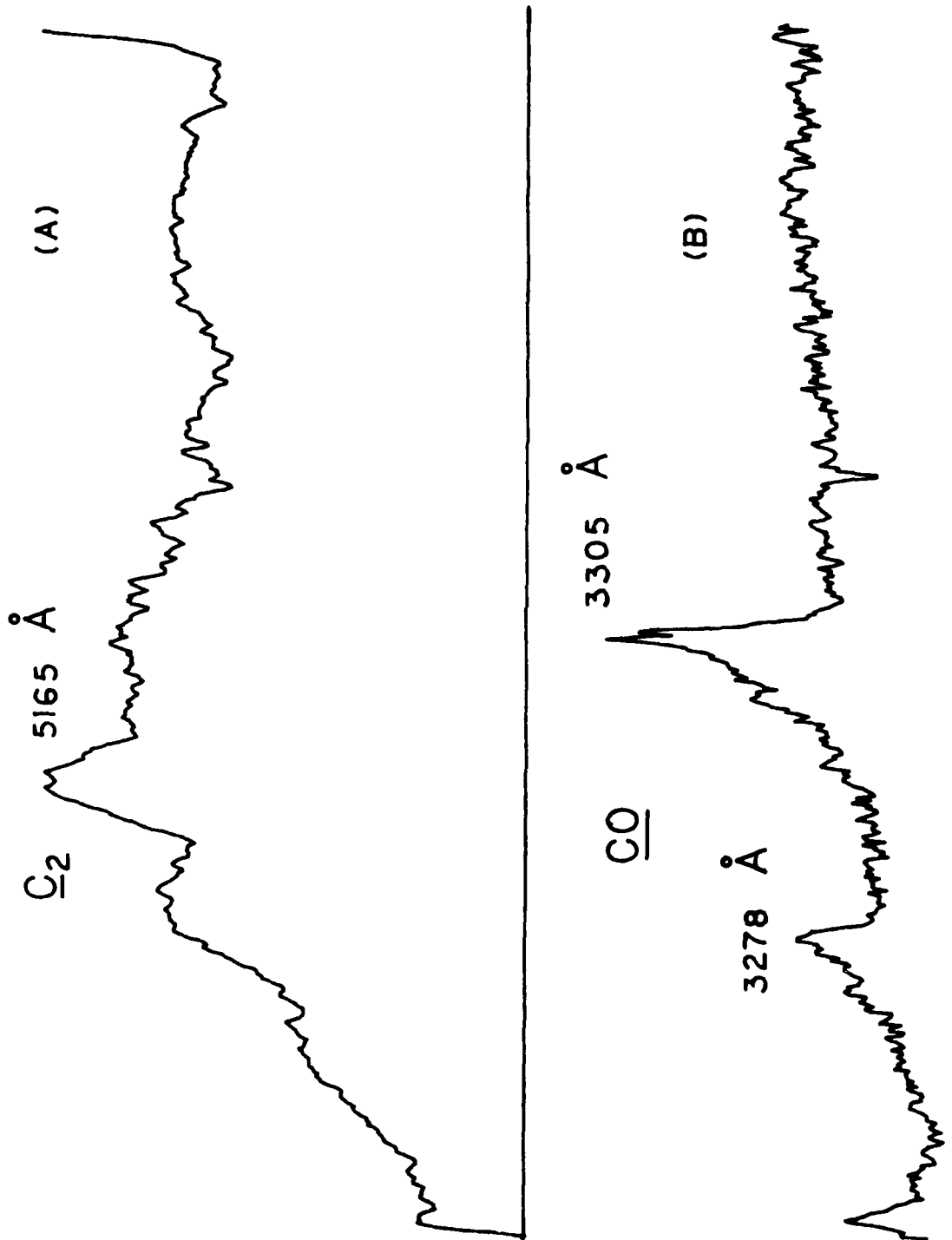
Figure 10. C_2 and CO emissions from propellant combustion
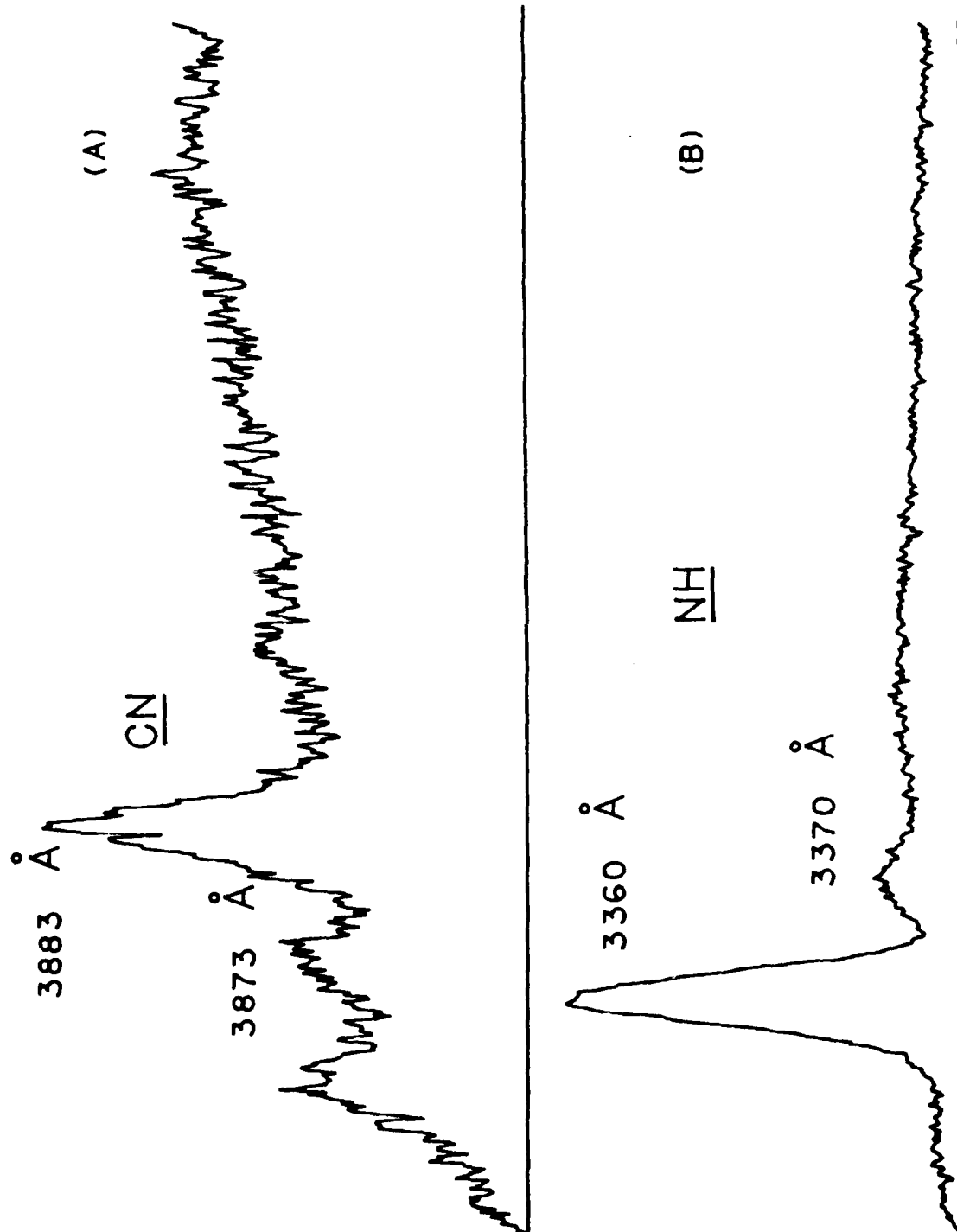
Figure 11. CN and NH emissions from propellant combustion

Table 3: Some reactive species in propellant flames*

	LOVA-1	LOVA-2	NOSOL	Pb-NOSOL	DB-1
C_2	yes	yes	–	yes	yes
CH	no	no	no	no	no
CN	yes	yes	–	yes	yes
CO	–	yes	–	yes	yes
N_2	yes	no	–	yes	no
NH	yes	yes	–	yes	yes
NO	–	no	–	–	no
OH	no	in O_2 atm	–	–	in O_2 atm

* Other possible species: CH^+, CO^+, and HCO or HNO_2.

their electron. However, if the flame contains some metallic impurity, then ionization becomes more likely. In fact, the sodium-doublet at 5891 Å has shown up very strongly in the NOSOL and Pb-NOSOL flames. Copper may have been detected as CuCl by strong bands at 4755 Å in the DB-1 flame, and at 4330 Å and 4354 Å in the LOVA-1 flame.

Because this work was initially focused on those reactive species and flame products derived from the major propellant components such as NC and RDX, no serious attempts were made to search for metal species in the gas phase. Therefore, the presence or absence of any metals and ions in the flames is still unknown.

Effects of O_2 On Flame Emissions

As reported earlier, a significant finding in this work is the complete absence of the OH signal when the propellants were burned in argon or nitrogen. However, OH was detected readily when the LOVA and DB propellants were burned in air or in Ar/O_2 mixtures. An example is shown in Figure 12. In such situations, the OH emission occurred immediately after ignition. Its intensity was strong throughout the combustion, indicative of the abundance of OH in all the combustion zones.

The Third Positive CO band was also affected by the presence of O_2 in the buffer gas. Experiments were carried out at 14 atm (~200 psi) of Ar/O_2 mixtures, in which the accumulated peak-intensity at 3304 Å, I_{total}, was measured as a function the initial oxygen content. The results listed in Table 4 clearly show that O_2 did not deplete the amount of CO by oxidizing it to the final product CO_2 as first thought; on the contrary, it contributed to the CO formation.

Table 4. Accumulated peak-intensity of CO band at 3304 Å

% O_2 in Ar	I_{total} (10^3 counts)
0	1.5
5	4.5
10	16.5
20	27.9

25
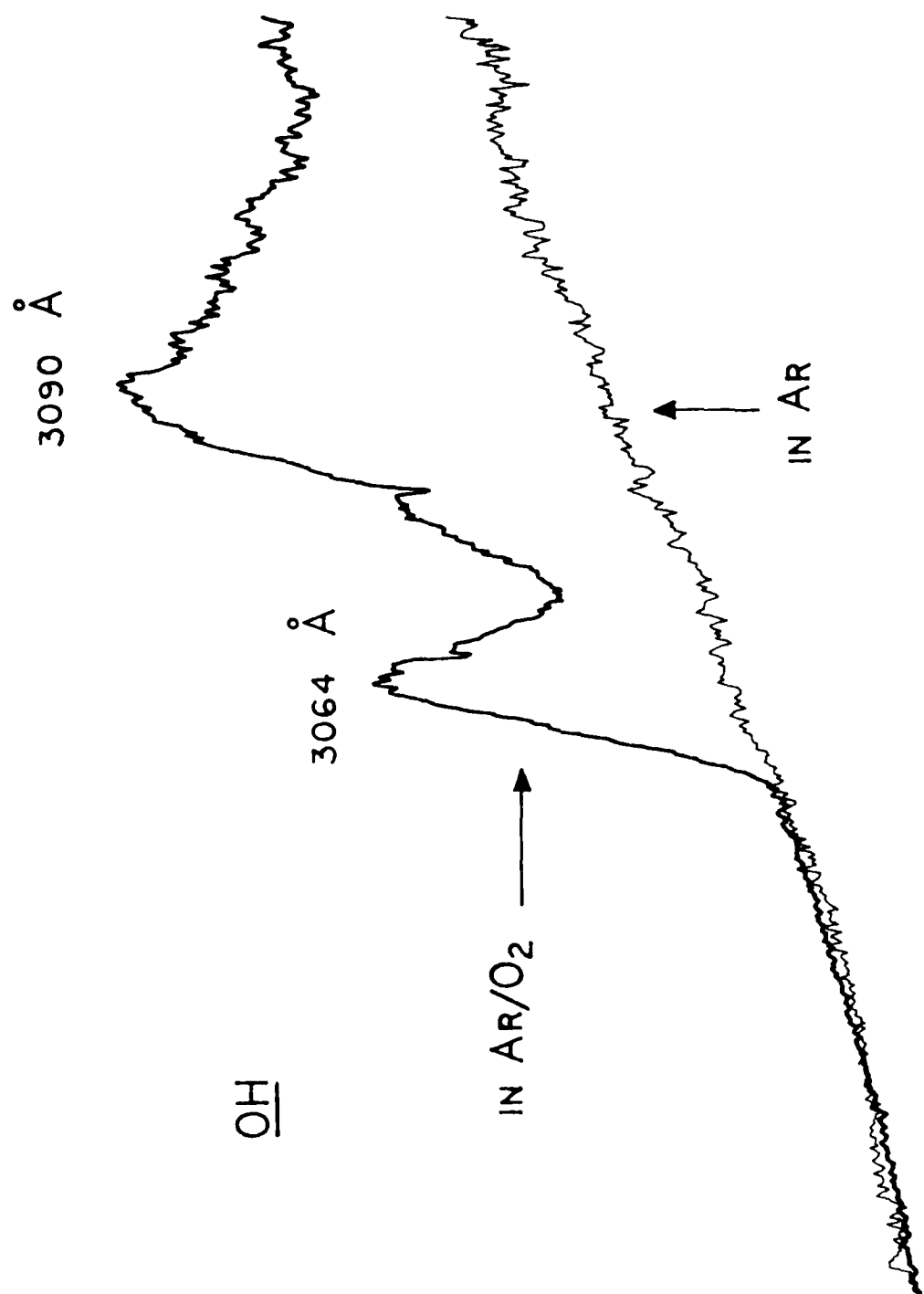
Figure 12. OH emission from DB-1 combustion in Ar/O$_2$ atmosphere

3500   3600 Å   3675

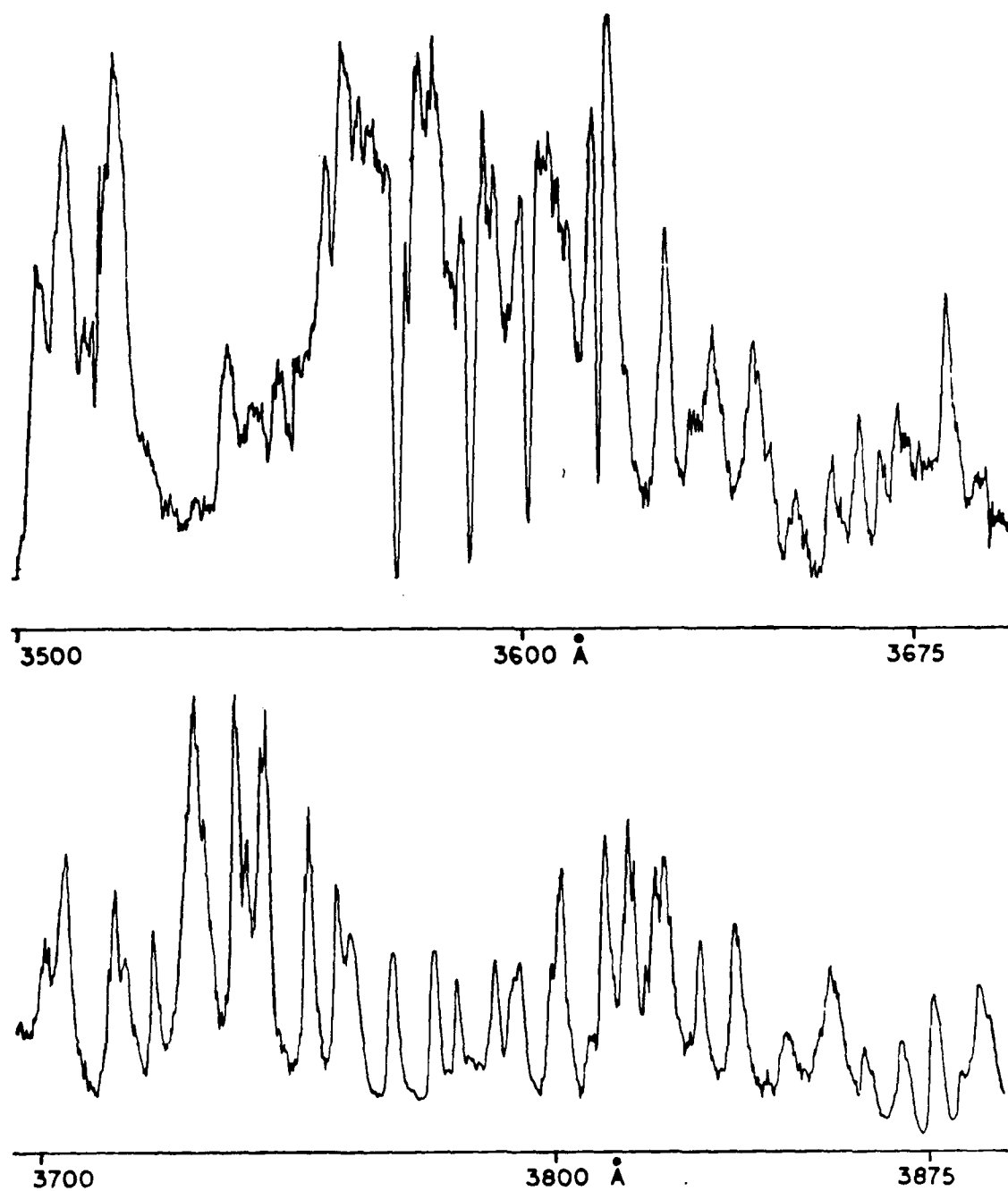3700   3800 Å   3875

Figure 13. Early emission from DB-1 combustion in the 3500-3900 Å
region

27

Early Emission from NC/NG Flame

During the search for emissions in the region below 4000 Å, a series of well-structured bands was found very early in each burning of the DB-1 propellant in argon and in nitrogen. The pressure at which this series occurred was about 12-14 atm (~170-200 psi). Figure 13 shows the series consisting of sharp lines, regularly spaced at intervals of 5 to 10 Ångstrom. The relative line intensities also exhibit a periodic trend. The duration of this emission series is very brief; by a rough estimate, it lasted no longer than a millisecond. Therefore, the source of this spectrum must be a highly reactive species. At higher pressures, when the dark zone vanishes, so does the spectrum. The reactive emitters must be some dark zone species.

Only qualitative speculations about the source of this spectrum can be made at the present time. Calculated transitions for a number of diatomic flame species failed to match the emission lines found here. Hydrocarbon flame bands in the 3200-4000 Å were obtained in the oxyacetylene flame, and may be due to HCO (Ref. 22). However, its regular structure does not quite match the emission peaks found in this work. Another possibility is HONO, with electronic transitions in the same spectral range (Ref. 23). Unfortunately, not enough information regarding the excited states of this molecule is available to calculate the rotational-vibrational lines in its electronic emissions.

It is also possible that this is an overlap spectrum from more than one source. Even if this early emission were from a single source, the band head of the series has not been reached yet. For a complete spectrum, further search will have to be carried toward shorter wavelengths.

DISCUSSION

Propellant Combustion in Inert Atmospheres

The order of the overall flame reaction has been determined for some propellants. The NOSOL propellants exhibit a second order flame chemistry. A simple guess would be a reaction between an aldehyde and NO_2. However, emission studies done here in pure argon have shown the presence of CN and NH, and no signs of CH and OH. This could imply a combustion with a predominantly RCN-type fuel flame (Refs. 17, 20). Thus, a reasonable hypothesis here should include RCN:

$$n_{f1} \cdot RCHO + n_{f2} \cdot R'CN + n_o \cdot NO_2 \rightarrow \text{Final Products} \qquad (I)$$
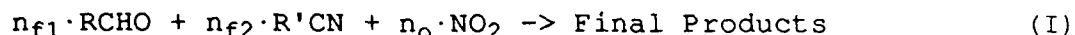
with the stoichiometric coefficients $n_{f1} + n_{f2} + n_o \sim 2$. This overall reaction is applicable to the DB propellants as well, based on the similarity in primary ingredients between the NOSOL and DB propellants, and also because of the same spectroscopic findings in both cases.

The flame chemistry of the LOVA propellants follows a third order reaction. Thus a smaller effect on the heat feedback to the condensed phase partly explains the lower burning rate of LOVA compared to the nitrate ester propellants. Since aldehydes, HCN, NO_2 and N_2O often count among the major components of nitramine flames (Refs. 7, 15, 21), the following general scheme is proposed for the LOVA flame:

$$n_{f1} \cdot RCHO + n_{f2} \cdot R'CN + n_{o1} \cdot NO_2 + n_{o2} \cdot N_2O \rightarrow \text{Final Products} \qquad (II)$$
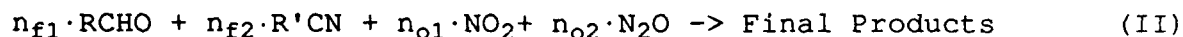
with $\Sigma_i n_{fi} + \Sigma_i n_{oi} \sim 3$. The stoichiometry in Reactions I and II can be established only after the major elementary reactions have been defined.

A common aspect found in all the flames is the pervasive C_2 Swan-bands in their emissions. This suggests that the propellant combustion act as fuel-rich flames, producing carbonaceous fibers seen on the propellants during and after the burnings. This fuel-rich model is particularly most applicable to the LOVA flame where, as noted earlier, smoke was observed during the burnings in argon.

Neither NO emission nor CH emission was detected. The failure to find emissions by a species does not necessarily discount its existence. It could also mean that the molecule or radical was produced in its ground state and would be better detected by absorption, or it could have escaped detection through reactive channels. Considering the early emissions by CO at 4661 and 5198 Å, and NH at 3360 Å, the following reactive channel seems to be the case for those missing CH and NO bands:

$$CH + NO \rightarrow CO + NH + 462.3 \text{ kJ/mole} \qquad (III)$$
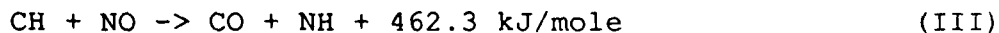
Other similar reactions could also be written to account for the CO-formation. However, such arguments would need time-resolved monitoring of both reactants and products for supporting evidence.

Effect of Ambient O_2

The presence of oxygen in the atmosphere has its strongest influence on the burning rate at low pressures only. The burning rate at high pressures is almost the same in reactive atmospheres as in inert gas. Thus, heat exchange between the flame and the propellant becomes the dominant factor controlling the high-pressure burning rate. It is clear that there are two different processes competing to affect the burning rate in the presence of oxygen: heat feedback from all the reactions in the gas phase, and reactions of O_2 which directly accelerate the propellant decomposition.

Reactions in the Gas Phase

There are at least two reactions between oxygen and the flame species. As an explanation of the strong OH emission in the O_2-supported burnings of the DB-1 and LOVA propellants, the following reaction is postulated:

$$CH + O_2 \rightarrow CO + OH + 512.9 \text{ kJ/mole} \qquad (IV)$$
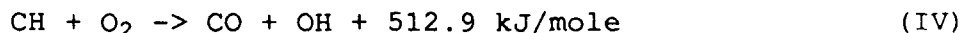
This agrees with the rise in the total CO emission intensity at 3304 Å in the DB-1 flame as more O_2 is added to argon. The energy balance in Reaction IV contributes to the heat needed for faster decomposition of nitrocellulose and nitroglycerin.

Other exothermic reactions involving O_2 in the gas phase near the edge of both the burning surface and the flame may have been partly responsible for flame spreading in the LOVA combustion.

Reactions at the Surface

The measurements of the burning rate at low pressures of Ar/O_2 mixtures have shown that the degradation at the burning surface is less pressure-dependent than in the cases of inert atmospheres. This smaller pressure-dependence translates into a smaller dependence on the heat transfer from the gas phase processes. Similarly, Kubota has found that the burning rate of RDX and HMX propellants depends largely on the heat released by the surface reactions, and to a negligible extent on

the energy feedback from the luminous flame (Ref. 24). In the experiments with Ar/O$_2$ done here, the factor controlling the burning rate at low pressures may not be so much the heat released by the surface as the direct reactions between O$_2$ and the burning surface, whether that surface be solid or liquid. The small Ar/O$_2$ flow rate which maintained the low pressure in the combustion chamber during each experiment could have allowed a long enough residence-time for O$_2$ to interact with the burning surface.

Another sign of O$_2$-induced decomposition at the surface is again the very early appearance of OH. Although reaction IV produces OH and CO, the CO emission at 3304 Å and the first OH appearance did not happen at the same time. In fact, the OH signal was seen immediately after ignition and lasted throughout the burning process. Thus, Reaction IV is only one of the steps giving OH. A high-temperature reaction of O$_2$ with RDX or nitrocellulose/nitroglycerin can account for the early formation of OH.

Because of the complex nature of the RDX and nitrocellulose molecules, only a general scheme of the postulated reactions with O$_2$ is given here:

The main point here is that O$_2$ helps break up the remaining rings after one or more NO$_2$-groups have been removed and, in the process, produces OH and other intermediates.
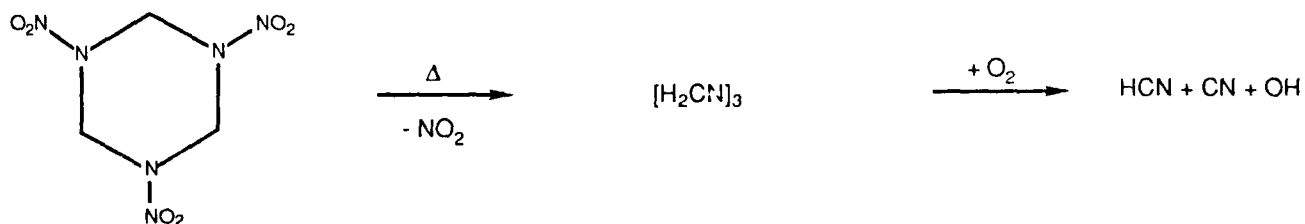
CONCLUSIONS

In this survey study, the burning rate for a variety of nitramine and nitrate ester propellants has been determined as a function of pressure and composition of the surrounding atmosphere. A number of reactive species have been identified in the propellant flames. The findings from all the propellants studied in this work are indicative of a rich flame with the characteristics of a predominantly RCN-type fuel. The flame chemistry follows second- and third-order rates for the nitrate ester and nitramine propellants, respectively. However, the stoichiometry of these flames still needs to be worked out in order to evaluate the energy balance from the combustions.

Results from the experiments in both inert and reactive atmospheres show two competing processes which affect the propellant burnings. At low pressures, the presence of O_2 is dominant on the burning rate and makes it less dependent on the flame-reactions. This suggests a possible O_2-chemistry at or near the condensed surface. At high pressures, the burning rate is mostly controlled by the heat feedback from the flame, and any chemistry involving O_2 becomes negligible in effect.

While a number of gas phase reactions, with and without O_2, have been determined which provide a glimpse at the flame chemistry of the propellants, some other processes are based more on speculations. Such is the case of the exothermic heterogeneous reactions at the burning surface, postulated here to partly account for the early OH formation. These heterogeneous events could be the major factors controlling the burning rate at low pressures, when the flame reactions are too slow and too far from the condensed phase to affect it.

RECOMMENDATIONS

This work has shed some light on the general aspects of propellant combustion. Still, there are many unanswered questions. Although the most obvious problem is the stoichiometry of the flame chemistry, many details must first be gathered to put together the overall picture:

-The first task is to enumerate all the major flame participants. There should be many more reactive transients than have been found in this work. Many intermediates may have been formed in their electronic ground states and can be detected only by absorption or laser-induced fluorescence (LIF). Moreover, the presence of impurities in the propellant and their significance in the flame, such as inducing ionization, should be checked out. The 3500-3900 Å spectrum from the dark zone of the DB flame must be investigated further to identify its emitters.

-The second task is to determine the interactions between those major participants. The spatial and temporal distributions of the intermediate and final products of the propellant flames can help decide among the alternative mechanisms. In addition, the temperature-profile of a flame must be known. Not only does it serve as a guide to estimate certain energetic reactions; but the thermal gradients, and thus the heat-transfer rates, among the various flame zones can then be derived.

Those are some of the problems concerning the propellant combustion itself. Surely, the methodology required to address these problems can also be improvised. The LIF technique can help determine the reactive intermediates. The CARS method, which has proved valuable in monitoring the equilibrium products of the air-supported LOVA-flame (Ref. 7), can be applied to high-pressure propellant combustion. The benefits with LIF and CARS in propellant studies have been widely discussed in the literature and need not be further debated here. Finally, a new design of the optical bomb should include a means to keep the flame stationary during the propellant burning. This will greatly improve the accuracy in plotting the species profile of the flame.

References

1. Harris, L. E., "Broadband N_2 and N_2O CARS Spectra from a CH_4/N_2O Flame", <u>Chemical Physics Letters</u>, Vol. 93, pp. 335-340, December 1982.

2. Harris, L. E., "CARS Spectra from Lean and Stoichiometric CH_4/N_2O Flames", <u>Combustion and Flame</u>, Vol. 53, pp. 103-121, November 1983.

3. Fendell, J., Harris, L. E. and Aron, K., "Theoretical Calculation of H_2 CARS Spectra for Propellant Flames", Technical Report ARLCD-TR-83048, ARDC, Picatinny Arsenal, NJ, December 1983.

4. Aron, K. and Harris, L. E., "CARS Probe of RDX Decomposition", <u>Chemical Physics Letters</u>, Vol. 103, pp. 413-417, January 1984.

5. Harris, L. E., "Reply to Comment on "CARS Probe of RDX Decomposition"", <u>Chemical Physics Letters</u>, Vol. 109, pp. 112-113, August 1984.

6. Haw, T., Cheung, W. Y., Chiu, G. C. and Harris, L. E., "A Study of Flame Species using CARS", <u>40th Symposium on Molecular Spectroscopy</u>, Abstract WH10, p. 106, June 1985.

7. Cheung, W. Y., <u>Combustions and Laser Diagnostics for Propellant Research</u>, Report No. GC-TR-85-183, Geo-Centers, Inc., Wharton, NJ, 1985.

8. Cheung, W. Y., <u>Optical Diagnostics for Propellant Research, Phase I Test Report, Part 1</u>, Report No. GC-TR-86-590, Geo-Centers, Inc., Wharton, NJ, 1986.

9. Cheung, W. Y., <u>Optical Diagnostics for Propellant Research", Phase II Test Report</u>, Report No. GC-TR-87-1590, Geo-Centers, Inc., Wharton, NJ, 1987.

10. Vu, T. H. and Field, R. "Propellant Combustion Study by Coherent Anti-Stokes Raman Scattering", <u>Advances in Laser Science - II</u>, American Institute of Physics, pp. 693-695, 1987.

11. Kuo, K. K. and Summerfield, M., <u>Fundamentals of Solid Propellant Combustion</u>, Progress in Astronautics and Aeronautics, Vol. 90, AIAA, Inc., New York, NY, 1984.

12. Fifer, R. A., "Workshop Report: Fundamental Reactions in Solid Propellant Combustion", Technical Report ARBRL-TR-02166, USA Ballistic Research Laboratory, Aberdeen, MD, May 1979.

13. Mal'tsev, V. M., Stasenko, A. G., Selezner, V. A., and Pokhil, P. F., "Spectroscopic Investigation of Combustion Zones of Flame Flares of

Condensed Systems", <u>Combustion, Explosion and Shock Waves</u>, Vol. 9 , pp. 186-190, March-April 1973.

14. Davidchuk, E. L. and Mal'tsev, V. M., "Infrared Spectral Investigations of the Combustion Zones of Nitroesters in a Vacuum", <u>Combustion, Explosion and Shock Waves</u>, Vol. 10, pp. 575-579, September-October 1974.

15. Fifer, R. A.,"Chemistry of Nitrate Ester and Nitramine Propellants", in <u>Fundamentals of Solid Propellant Combustion</u>, Progress in Astronautics and Aeronautics, Vol. 90, Chapter 4, AIAA, Inc., New York, NY, 1984.

16. Powell, E. G. and Wilmot, G. B., "Infrared Spectroscopic Studies of the Mechanism of Double-Base Propellant Combustion", <u>14th JANNAF Combustion Meeting</u>, Vol.1, CPIA Publication 292, pp. 163-178, December 1977.

17. Edwards, T., Weaver, D. P., Campbell, D. H., and Hulsizer, S., "Investigation of High Pressure Solid Propellant Combustion Chemistry Using Emission Spectra", <u>AIAA J. Propulsion and Power</u>, Vol. 2, pp. 228-234, May-June 1986.

18. Siddiqui, K. M. and Smith, I. E., "Flame Spreading Phenomena in Double-Base Propellants", <u>Combustion and Flame</u>, Vol. 25, pp. 335-341, December 1975.

19. Kubota, N., Ohlemiller, T. J., Caveny, L. H., and Summerfield, M., <u>The Mechanism of Super-Rate Burning of Catalyzed Double-Base Propellants</u>, Report 1087, Princeton University, Aerospace and Mechanical Sciences Dept., Princeton, NJ, 1973.

20. Miller, J. A., Branch, M. C., Chandler, D. W., Smooke, M. D., and Kee, R. J., "The Conversion of HCN to NO and N_2-O_2-HCN-Ar Flames at Low Pressure", <u>20th Symposium (International) on Combustion</u>, pp.673-684, Combustion Institute, 1985

21. Schroeder, M. A., "Critical Analysis of Nitramine Decomposition Data: Product Distribution from HMX and RDX Decomposition", <u>18th JANNAF Combustion Meeting</u>, Vol. 2, CPIA Publication 347, pp. 395-413, 1981.

22. Hornbeck, G. A. and Herman, R. C., "Hydrocarbon Flame Spectra", <u>Industrial and Engineering Chemistry</u>, Vol. 43, pp.2739-2757, December 1951.

23. King, G. W. and Moule, D., "The Ultraviolet Absorption Spectrum of Nitrous Acid in the Vapor State", <u>Canadian Journal of Chemistry</u>, Vol. 40, pp.2057-2065, December 1962.

24. Kubota, N., "Combustion Mechanism of Nitramine Composite Propellants", _18th Symposium (International) on Combustion_, The Combustion Institute, pp. 187-194, 1981.

DISTRIBUTION

Commander
Armament Research, Development and
Engineering Center
U.S. Army Armament, Munitions and
Chemical Command
ATTN: SMCAR-IMI-I (5)
      SMCAR-AEE, J. A. Lannon (3)
      SMCAR-AEE-B, D. S. Downs
      SMCAR-AEE-BR, Y. Carignan
      A. J. Beardell
      A. Bracuti
      R. Field (2)
      L. Harris
Picatinny Arsenal, NJ 07806-5000

Commander
U.S. Army Armament, Munitions
and Chemical Command
ATTN: AMSMC-GCL (D)
Picatinny Arsenal, NJ 07806-5000

Administrator
Defense Technical Information Center
ATTN: Accessions Division (12)
Cameron Station
Alexandria, VA 22304-6145

Director
U.S. Army Materiel Systems
Analysis Activity
ATTN: AMXSY-MP
Aberdeen Proving Ground, MD 21005-5066

Commander
Chemical Research, Development
and Engineering Center
U.S. Army Armament, Munitions
and Chemical Command
ATTN: SMCCR-MSI
Aberdeen Proving Ground, MD 21010-5423

Commander
Chemical Research, Development
and Engineering Center
U.S. Army Armament, Munitions and
Chemical Command
ATTN: SMCCR-RSP-A
Aberdeen Proving Ground, MD 21010-5423

Director
Ballistic Research Laboratory
ATTN: AMXBR-OD-ST
Aberdeen Proving Ground, MD 21005-5066

Chief
Benet Weapons Laboratory, CCAC
Armament Research, Development and
Engineering Center
U.S. Army Armament, Munitions and
Chemical Command
ATTN: SMCAR-CCB-TL
Watervliet, NY 12189-5000

Commander
U.S. Army Armament, Munitions and
Chemical Command
ATTN: SMCAR-ESP-L
Rock Island, IL 61299-6000

Director
U.S. Army TRADOC Systems
Analysis Activity
ATTN:ATTA-SL
White Sands Missile Range, NM 88002

Director
Industrial Base Engineering Activity
ATTN: AMXIB-MT (2)
Rock Island, IL 61299-7260

Director
U.S. Army Material Technology
Laboratory
ATTN: SLCM-IML
Watertown, MA 02172

Dr. Robert W. Shaw
Army Research Office
Research Triangle Park, NC 27709-2211

Dr. Carl Melius
Division 8357
Sandia National Laboratories
Livermore, CA 94551-0969

Dr. Celeste Rohlfing
Division 8341
Sandia National Laboratories
Livermore, CA 94551-0969

Geo-Centers, Inc. (5)
7 Wells Avenue
Newton centre, MA 02159